Investigations on the Adhesion and Interfacial Properties of Polyurethane Foam/Thermoplastic Materials

Nasir Mahmood, Karsten Busse, Jörg Kressler

Fachbereich Chemie, Martin-Luther-Universität Halle-Wittenberg, D-06099 Halle (Saale), Germany

Received 2 September 2005; accepted 24 July 2006
DOI 10.1002/app.25179
Published online in Wiley InterScience (www.interscience.wiley.com).

ABSTRACT: The adhesion and interfacial properties of polyurethane (PU) foams with thermoplastic (TP) materials were investigated using different techniques. The adhesion performance of PU foam with TP materials was evaluated using the peel test method, and the adhesion durability was checked after different climate treatments. X-ray photoelectron spectroscopy (XPS), atomic force microscopy (AFM), and contact angle measurements were used to study the surface and interface morphology of PU foam and TP material system. Three types of PU foam samples which differ in their composition and also five commercially available TP blends systems, based on poly(carbonate), poly(styrene-*co*-maleic anhydride), poly(acrylonitrile-butadiene-styrene), and silicone acrylate rubber have been used. The slow reacting foam shows the best adhesion properties with all the TP materials. The climate treatments strongly effected the PU foam adhesion durability with poly(carbonate) containing TP materials (70–80% loss in adhesion), but nearly no effect with poly(styrene-*co*-maleic anhydride). The samples with lowered adhesion could be separated by peeling without visible foam residues on the TP surface. AFM, XPS, and surface tension studies have shown that the surface properties of the TP material are still governed by the PU foam. © 2007 Wiley Periodicals, Inc. J Appl Polym Sci 104: 479–488, 2007

Key words: adhesion; polyurethanes; thermoplastics; interfaces; foams

INTRODUCTION

The polyurethane (PU) foams are cellular or expanded materials synthesized by the reaction of diisocyanate with polyol in the presence of a blowing agent. According to their mechanical properties, PU foams are either categorized as flexible, rigid, or semirigid material. PU foams are multi block copolymers considered as consisting of alternating hard and soft segments.[1] The soft segments are composed of long chain polyethers or polyesters, which exhibit flexibility (low T_g part) and elastomeric properties at room temperature. The hard segments consist of hydrogen bonded urea and urethane linkages, which are formed by the reaction of isocyanate with water and the OH group of the polyol (high T_g part).

The surface properties of materials play an important role in establishing a strong adhesive joint between adhesive and adherend. Several techniques such as atomic force microscopy (AFM), X-ray photoelectron spectroscopy (XPS), and contact angle measurements are well established for characterizing the chemical structure of different material surfaces.[2–4] These techniques have been applied to the investigations of the surface molar mass, impurities and end groups[5–9] specific interactions of surface groups,[10] and quantitative analysis of polymers.[11,12] The nature of the polar material to segregate at an interface is well known,[13] and this characteristic is important in the anchoring of molecules to solid substrates. The interaction with a substrate will be influenced by the chemical nature of the surface groups and leads to significant modification of the properties of the solid surface. Similar surface groups can attach themselves to the polymer air interface, and produce the modification of the surface, as a consequence of the difference in the surface free energy between the end and the main segment of the chain. The degree to which the surface groups cover the surface will be controlled by the surface free energy differences between end groups and backbone segments, the relative volumes of these elements, and the competing change in the free energy caused by forming a concentration gradient near the surface.

To enhance the adhesion between two materials, several methods like using primer or performing plasma treatment can be applied, but for industrial processes it is of interest to reduce the number of production steps. In this study we have investigated the adhesion and its failure of PU foams, which were directly applied on thermoplastic material systems. The adhesion properties were measured using the peel test method and the surface and interfacial properties were investigated using AFM, XPS, and contact angle techniques. The peel test is one of the most suc-

Correspondence to: K. Busse (karsten.busse@chemie.uni-halle.de).

Journal of Applied Polymer Science, Vol. 104, 479–488 (2007)

cessful test methods for assessing the interfacial adhesion force of flexible materials,[14–16] such as those used in the automotive and packaging industries. Many researchers have therefore extensively studied it and a large amount of experimental and theoretical work exists on this method of material testing.[14,17–21]

In our investigations, PU foam based on 4,4′-diphenylmethane diisocyanate (MDI), OH-terminated poly(ether), and H_2O as indirect blowing agent was foamed in contact with TP material systems, being commercially available blends of poly(carbonate) (PC), poly(styrene-*co*-maleic anhydride) (SMA), poly(acrylonitrile-butadiene-styrene) (ABS), silicone acrylate rubber (SAR), and glass fibers (GF). An aging of the system was simulated by a thermal treatment under defined humidity conditions. As after this treatment, nearly all of the samples have shown an adhesive failure during peel test, the separated surfaces from the PU–TP interface could be investigated in more detail. A previous article[22] described the internal structure of the PU foam at the interface.

EXPERIMENTAL

Materials

All the chemicals for PU foam and the TP material plates were used as obtained. MDI with an isocyanate index of 88 (isocyanate index is the molar ratio of isocyanate versus active hydrogen bearing groups, i.e., hydroxyl and amino groups) was used. The OH- terminated poly(ether)s were polypropylene and polyethylene oxide based with a weight ratio of 80 : 20 (PPO : PEO). Three different PU formulation were used (PU-a, PU-b, and PU-c), all of them forming a closed cell structure, and their details are given in Table I. Because of different catalysts and crosslinkers, the foam systems can be described as slow (PU-a), intermediate (PU-b), and fast (PU-c).[22–25]

The five types of thermoplastic material plates (prepared by compression molding with a size of 10.5 $\times$ 15 $\times$ 0.3 cm^3) used for the experiments are neat SMA (Cadon DMC250), a blend of PC with ABS (PC/ABS, Bayblend T65), a blend of PC with ABS and SMA (PC/ABS-SMA), and two samples reinforced with glass fibers, based on a blend of PC with ABS (PC/ABS-GF, Bayblend T88-2*N*, includes 10% glass fiber) and on a blend of PC with SAR (PC/SAR-GF).

TABLE I
Formulation Details of PU Foam Systems

Foaming system	Polyol (g)	Isocyanate (g)	H_2O/D_2O (g)
PU-a	100	45	2.6
PU-b	100	44	2.8
PU-c	100	54	3.1

Preparation of PU foam samples

To prepare the samples with PU foam adhered to TP material plate, an appropriate amount of polyol was mixed with MDI and mechanically stirred for some seconds. Finally, the reacting mixture was transferred to a heatable quadratic foaming tool (size: 20 $\times$ 20 $\times$ 2 cm^3), which already contains the TP material plate (size: 18 $\times$ 10 $\times$ 0.5 cm^3). The amount of PU educts was chosen depending on the composition to obtain a final product with a foam density of 0.16 $\pm$ 0.02 g/cm^3. The tool was then closed to allow the process to progress for 10 min at 40°C. After that the foamed plate was removed from the foaming tool.

To simulate aging of the junction between the TP and the PU foam, a climate treatment was performed by placing some samples in a climate chamber (Climats/Sapratin, St Médard d'Eyrans, France, Model: Excal 2221 HA). At 80% relative humidity (RH), these samples were heated within 1 h from room temperature to +80°C, stored for 4 h at this temperature, and afterwards cooled down within 2 h to −40°C, again stored for 3 h and finally heated up in 1 h back to room temperature. A single cycle takes therefore 11 h, and the complete thermal treatment contains 24 repeated cycles.

Peel test

The peel test samples were prepared by cutting the TP plate after the foaming process into rectangular strips of dimensions of 120 $\times$ 18 mm^2 with a 5-mm thick PU foam layer on it. The peel test was carried out by peeling the PU foam layer from TP material surface at a peel angle of 90° and at room temperature conditions as shown in Figure 1. The test uses the peel test fixture and computerized Zwick 1120 Werkstoffprüfmaschine (Zwick Roell, Ulm, Germany). The testing machine provides a constant rate of peel and continuously measures the force of detachment during the test. The peel fixture consists of a moving base and a holding point fixed to the testing machine. The peeling rate used was 10 mm/min. The peeling force P required for separating the PU foam layer from the TP material substrate was recorded continuously. The normalized total force G is related to the applied steady state peel load, P, the width, b, of the specimen and the peel angle, θ, by eq. (1).[21]

$$G = \frac{P}{b}(1 - \cos\theta) \quad (1)$$

The value of G includes the interfacial adhesion strength, and any plastic work done in bending the peel arm, which can be neglected in our measurements. The value of interfacial adhesion strength is assumed to be a characteristic of the particular inter-

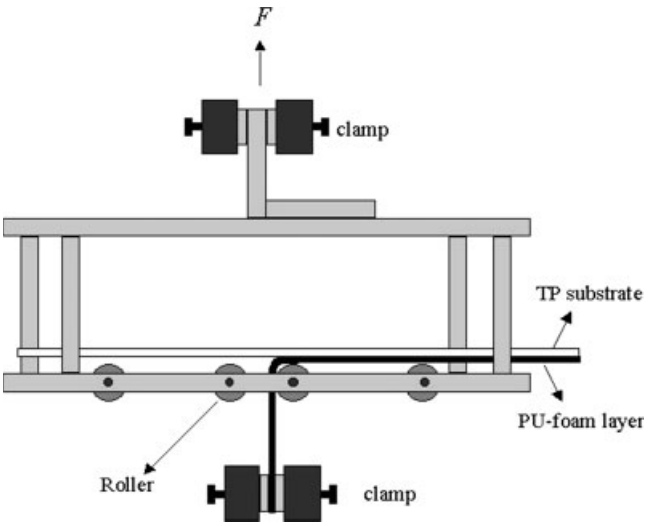

Figure 1 Schematic representation of peel test arrangement. A flexible PU foam layer was peeled from rigid TP material plate at a peel angle of 90°. The peel rate supplied from the instrument was 10 mm/min.

face, and ideally independent of the geometrical details of the peel test specimens such as the thickness of the peel arm and the peel angle. For each TP material system, five sample strips were measured to calculate a statistical error.

X-ray photoelectron spectroscopy

The surface chemical composition was determined by XPS using a ESCALAB iXL 220 spectrometer from Thermo-VG scientific (Datacomp Scientific, Toronto, Canada) operating at a pressure in 1×10^{-8} to 1×10^{-10} mbar range, equipped with an Al/Mg twin anode. Spectra were recorded at a takeoff angle of 30° and with a pass energy of 100 eV for survey scans. For each sample, a detailed scan of the O1s, C1s, N1s, and Si2p lines was performed with a step width of 0.1 eV and pass energy of 20 eV. The calibration of the binding energy (BE) scale was made by setting the C1s BE of the neutral carbon (C—C and C—H bonds) peak at 284.6 eV. The C1s and O1s were resolved into individual Gaussian peaks.

Atomic force microscopy

For AFM measurements, a Digital Instruments Industries multimode atomic force microscope (Veeco, Santa Barbara, CA) equipped with a nanoscope III controller was used. The images were acquired in taping mode with a resonant oscillating frequency of 300 kHz and a microfabricated silicone cantilevers of spring constant 15 N/m at ambient pressure, room temperature, and relative humidity conditions (~ 40%). From the height images, the mean surface roughness (R_a) is calculated.

Contact angle

The contact angle was obtained by observing a drop on the tested surface from the side with a Krüss G40 instrument (Hamburg, Germany) at a temperature of 20°C. The visible contact angles on both sides of the drop were measured. The surface tension or free energy (γ) is related to contact angle (θ) through Young's equation

$$\gamma_{sl} = \gamma_{sv} - \gamma_{lv}\cos\theta$$

where subscripts s, l, and v stand for solid, liquid, and vapor, respectively. Together with the geometric mean method defined by Good and Girifalco[26,27]

$$\gamma_{sl} = \gamma_{sv} + \gamma_{lv} - 2\sqrt{\gamma_{sv}^d \gamma_{lv}^d} - 2\sqrt{\gamma_{sv}^p \gamma_{lv}^p}$$

the polar and disperse parts of the surface tension can be calculated using the geometric mean method of Owens, Wendt, and Rabel.[28]

$$\frac{\gamma_{lv}(\cos\theta + 1)}{2\sqrt{\gamma_{lv}^d}} = \sqrt{\gamma_{sv}^p}\sqrt{\frac{\gamma_{lv}^p}{\gamma_{lv}^d}} + \sqrt{\gamma_{sv}^d}$$

The testing liquids used to characterize the polymer surfaces through contact angle measurements were: bromonaphthalene[29] (fresh distilled prior to use), diiodomethane,[30] ethylene glycol,[29] glycerol,[29] formamide,[31] bidistilled water,[29] and a mixture of 30% ethylene glycol and 70% water[32] (EG/W = 30/70). The characteristic properties of these liquids are given in Table II. For every solvent, eight measurements were carried out and the mean value of the contact angle was calculated. The polar and disperse parts of the surface tension γ_{sv}^p and γ_{sv}^d were obtained as an average over all testing liquids.

As the foam samples obtained after peeling from the TP material are slightly bent, they cannot be used for this method. To measure the PU surface tension, the TP plate was replaced by a thin and flexible polyethylene (PE) sheet in the foaming tool. The sheet could be separated without bending the foam, as the adhesion was very low because of the nonpolarity of PE. Although the surface polarity is totally different to the other materials under investigation, the obtained results might give further information on the surface behavior of the PU foam.

RESULTS AND DISCUSSION

Adhesion properties

The adhesion strength measured in peel test is demonstrated in Figure 2. The *force* axis represents the force P required to peel and deform PU foam from

TABLE II
Characteristic Data of the Test Liquids Used for the Sessile Drop Studies

Test liquids	Source	γ_{lv}(mN/m)[a]	Polarity[a]	γ_{lv}^{d} (mN/m)[b]	γ_{lv}^{p} (mN/m)[c]
α-Bromonaphthalene	Aldrich[d]	46.60	0.0000	46.60	0.00
Diiodomethane	Merck[e]	50.80	0.0453	48.50	2.30
Ethyleneglycol	Merck[e]	47.70	0.3522	30.90	16.80
Glycerol	Merck[e]	63.40	0.4146	37.00	26.40
Formamide	Merck[e]	58.20	0.5070	28.69	29.51
EG/W = 30/70	Merck[e]	61.59	0.6672	20.50	41.09
Bidistilled water		72.80	0.7005	21.80	51.00

[a] See text for references.
[b] γ_{lv}^{d} is calculated by $\gamma_{lv}^{d} = \gamma_{lv} - \gamma_{lv} \times$ polarity.
[c] γ_{lv}^{p} is calculated by $\gamma_{lv}^{p} = \gamma_{lv} \times$ polarity.
[d] Munich, Germany.
[e] Darmstadt, Germany.

the TP material and the peeling length represents the length of PU foam stripe which was peeled from the TP material. The adhesion strength per unit width of sample strips was calculated according to eq. (1). The force due to the stretching and breaking of foam (region I and III in Fig. 2) was excluded. For each TP material plate, five samples were tested and an average value of the plateau II is reported as interfacial adhesion strength of a particular PU foam/TP material system.

Generally, three modes of failure have to be distinguished. Typical examples are depicted in Figure 3. The simplest case is the adhesive failure. The foam is removed from the TP material with nearly no visible foam parts remaining at the TP material surface. Only in that case, the obtained force corresponds to the adhesive failure. In the second case, the foam breaks without showing a typical plateau II in the peel test. These samples have been excluded from the average calculation, described above. The third case appears, when the PU foam has a very strong adhesion to the TP material. The foam is only partly removed from the surface during peeling, a more or less compact film remains at the surface, i.e., instead of an interfacial failure (with measurable adhesion force) only a breaking of the foam, parallel to the surface, appears. In that case, the adhesion strength at the PU foam/TP material interface must be higher than the measured cohesive failure strength of the PU foam bulk. The remaining PU film at the TP surface has a typical thickness of 0.1 mm. In the case of adhesive failure, the skin like layer remains on the foam side and forms a smooth, nonporous surface.

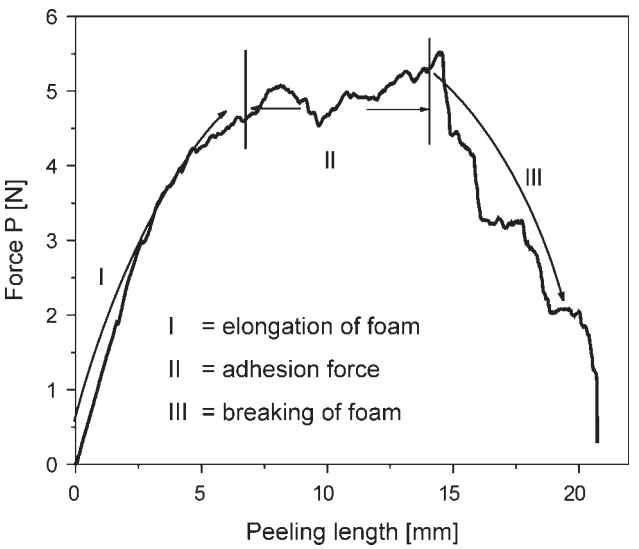

Figure 2 Peel test data obtained when an 18 mm wide and 2-mm thick PU-a foam sample was peeled at a peel rate of 10 mm/min from PC/ABS-SMA TP material before climate test using Zwick testing machine. The sections indicated by numbers I–III represent the elongation of foam, adhesive peeling of PU foam from TP material, and breaking of foam, respectively.

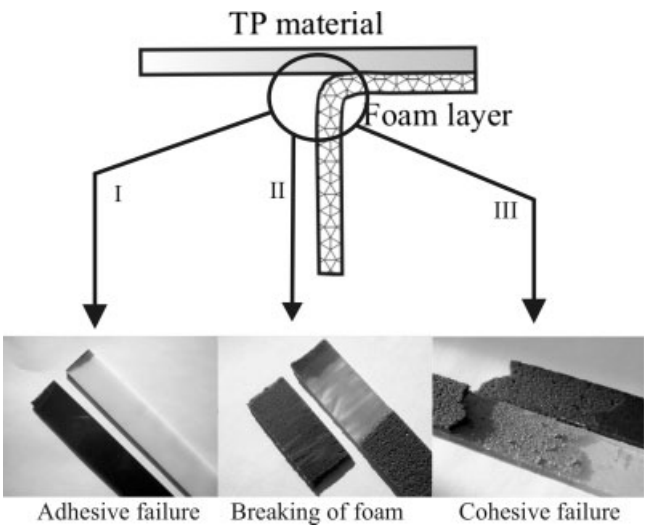

Figure 3 Schematic representations of modes of failure during peel test. The sections indicated by numbers I–III represent photographs of failed samples after adhesive failure (I), breaking (II), and cohesive failure (III) of PU foam (dark gray) from TP material plates (white or clear), respectively.

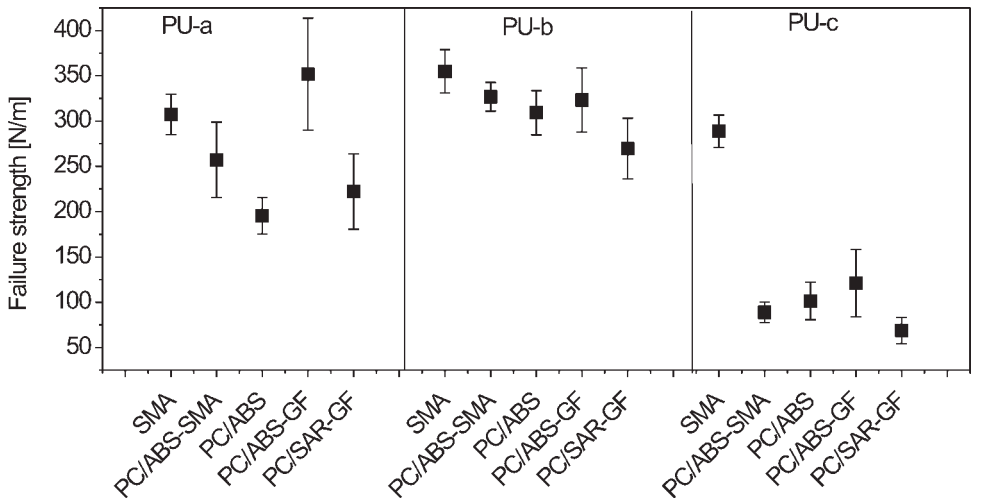

Figure 4 Failure strength of PU-a, PU-b, and PU-c foam systems with five different TP materials as measured by peel test method before climate treatment. Samples PU-a and PU-b show always, PU-c only with SMA cohesive failure, otherwise adhesive failure.

Adhesion performance before climate treatments

The peel test results of PU-a, PU-b, and PU-c foam systems with five different TP material samples before climate treatment are shown in Figure 4. Samples PU-a and PU-b show always, PU-c only with SMA cohesive failure, otherwise adhesive failure.

In case of cohesive failure, the measured failure strength should be independent of the TP material, but in case of the PU-a foam system, significant variations of the failure strength can be observed. The reason for this behavior can be found, when having a closer look at the remaining film on the TP surface. For PU-a foam with PC/ABS and PC/SAR-GF TP materials, the film was not totally remaining on the TP surface, some small parts (in the range of mm^2) were missing, as they remained at the foam side. The origin of this local effect might be due to some silicon oil at the TP surface, which lowers the adhesion and sometimes was observed at the TP surface.

For all other combinations of PU foam systems with TP material showing cohesive failure, there is no significant difference within the experimental error. Independently of the composition, the foam fails in the range of 300 ± 50 N/m.

With respect to the adhesion strength, the PU-c foam system behaves similar only with SMA, the adhesion with PC containing TP materials is significantly lowered. The reason for a good adhesion on SMA could be a reaction of maleic anhydride (component of SMA TP material) with MDI during the foaming process.[33] On the other hand, due to the composition of this foam system, the reaction is twice as fast

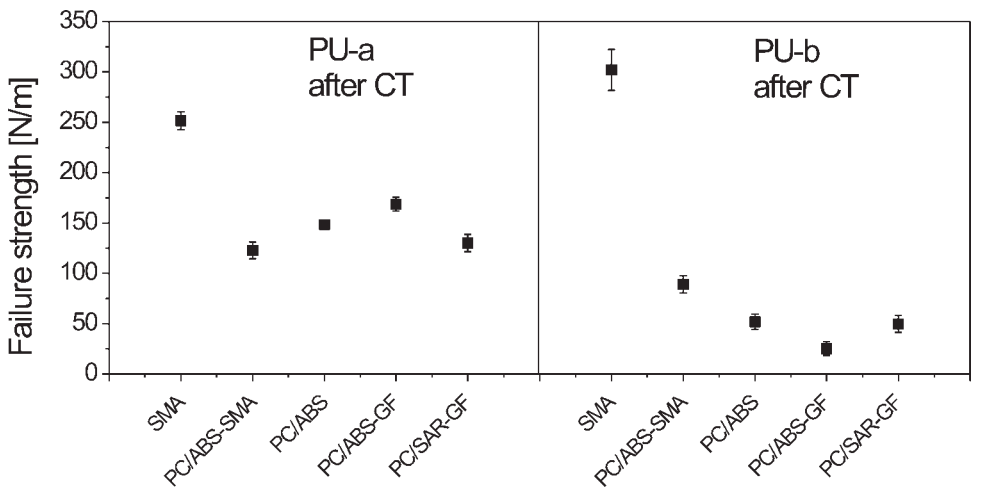

Figure 5 Failure strength of PU foam system with five different TP materials as measured by peel test method after standard climate treatment (RT to 80°C + 80% RH to −40°C for 24 cycles): (a) PU-a foam system, (b) PU-b foam system. Samples PU-a and PU-b show only with SMA cohesive failure, otherwise adhesive failure.

as in the other foam systems[22] and therefore, the formation of stable hydrogen bonds at the interface seems to be decreased. Because of the poor adhesion properties of PU-c foam system with PC containing TP materials, it was excluded from further adhesion durability studies like climate change experiments. The PU-a and PU-b foam systems have shown only cohesive failure during this test series, therefore the samples from these two foam systems were measured again after a climate treatment described earlier in the Experimental section.

Adhesion performance after climate treatments

The adhesion strength of PU-a and PU-b foam systems with five different TP samples was evaluated after different climate treatments and the results are depicted in Figure 5. The adhesion strength was strongly reduced after climate treatment in all the samples except the SMA TP material. In case of the SMA samples, once again cohesive failure occurred, and the loss of 10–15% failure strength must be due to an aging of PU foam material.

In PU-a foam system, the climate treatment reduced the adhesion failure strength of PU foam on PC containing TP materials to 140 ± 20 N/m. In PU-b foam systems, the adhesion failure appears at 55 ± 30 N/m. Because of the composition, the PU-a system was slowest during the reaction and PU-b had intermediate speed. Small differences between the TP materials can be observed, but no systematic dependence is deducible.

Therefore, it can be assumed, that in case of PC containing TP materials, the formed interface is mainly based on physical interactions like hydrogen bonding and that can be highly affected by water diffusion during climate treatments. Otherwise, as the connection between foam and SMA is not significantly affected by climate treatments, there seems to be a stronger interaction, e.g., a chemical linkage formed between MA and MDI.

Analysis of samples from PU foam/TP material interface

Atomic force microscopy

To investigate the effect of the PU adhesion on the TP material surface, the PC/ABS-SMA system was analyzed by AFM in more detail. In the AFM height image of neat PC/ABS-SMA TP material [Fig. 6(a)], some spherical particles of ~ 500 nm in diameter and

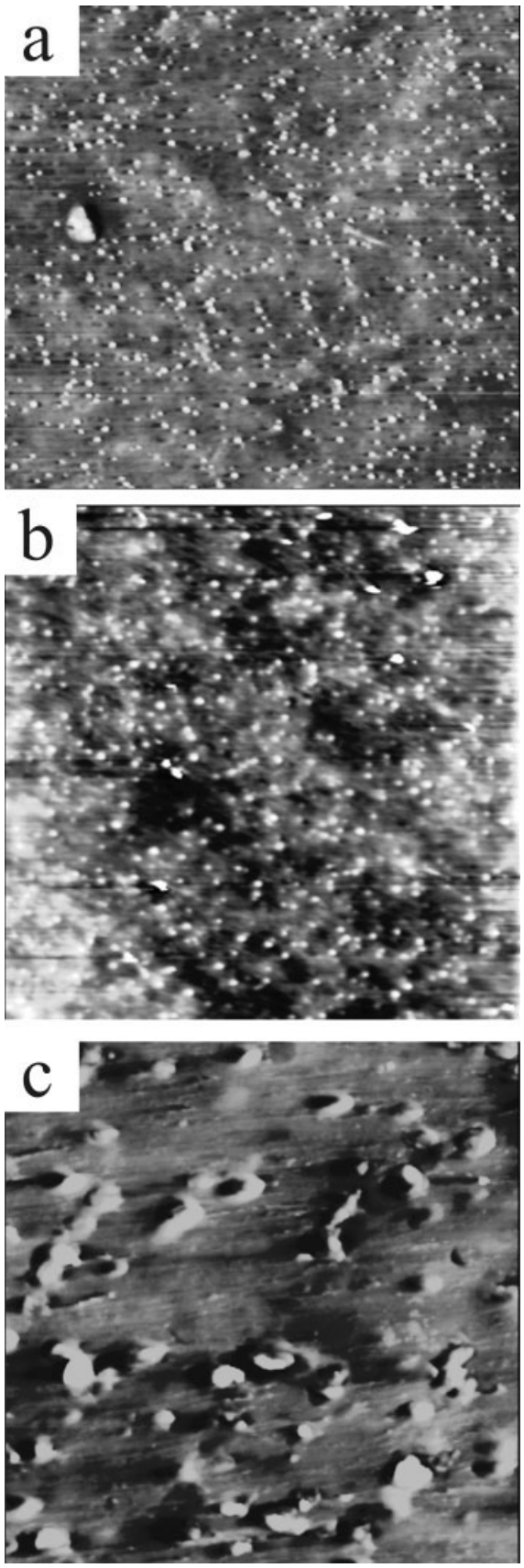

Figure 6 AFM height image of (a) neat PC/ABS-SMA TP material, (b) PC/ABS-SMA TP material from PU-b foam interface after climate treatment and peel test, and (c) PU-b foam after removing from PC/ABS-SMA TP material. The image size is 40 × 40 μm^2 for (a) and (b) and 10 × 10 μm^2 for (c).

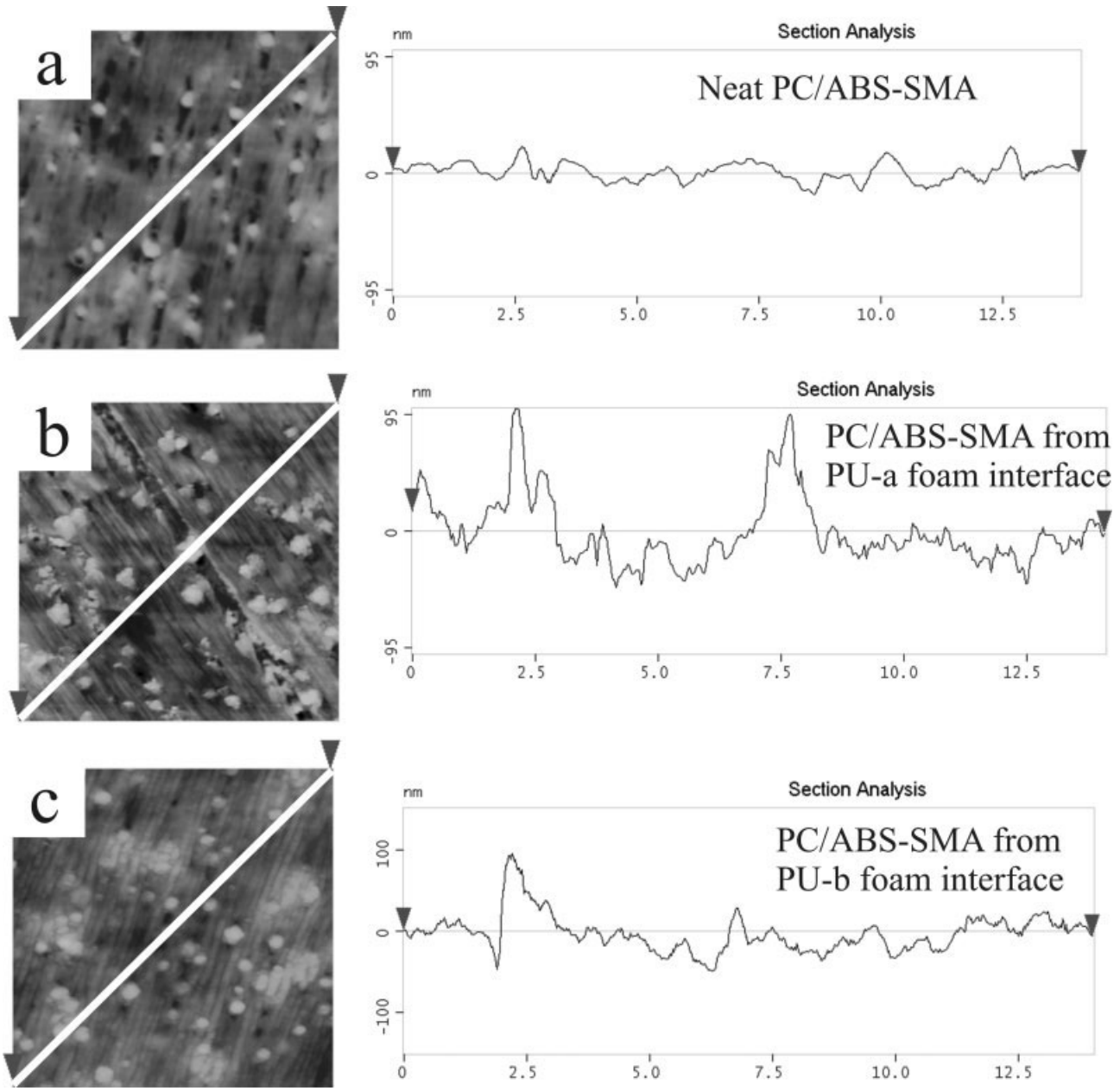

Figure 7 Cross-sectional line profiles of the AFM height images for: (a) neat PC/ABS-SMA, (b) PC/ABS-SMA TP material separated from PU-a, and (c) from PU-b foam interface, after climate treatment and peel test.

$\sim$ 100 nm in height [Fig. 7(b,c)] can be seen on the surface of TP material. These uniformly shaped spherical particles resemble the microstructure of classical rubber modified ABS grade,[34] and therefore belong mainly to the rubber phase of ABS. Because of the surface properties and polarity of PC component of TP material, the area occupied by PC [see background of Fig. 6(a)] appears larger than that expected from the overall composition. The surface roughness calculated from AFM height images and the corresponding section analysis plot for each material are depicted in Figure 7. The root mean square roughness of PC/ABS-SMA TP surface was determined to 7.5 nm for this sample. Keisler and Lataillade[35] and Sancaktar and Gomatam[36] have indicated the importance of surface roughness toward adhesion strength of materials, higher surface roughness means mechanical interlocking at the interface. But samples with high surface roughness (GF containing sample with an root mean square roughness >100 nm) have not shown better adhesion performance, which means that surface roughness is not the limiting factor for adhesion under the influence of climate conditions with high humidity.

Investigating the PC/ABS-SMA TP material surface after peeling the PU-b foam (after climate treatment

as adhesive failure is necessary), the same spherical particles with comparable size and distribution can be observed [Fig. 6(b)] however, the background of the sample surface in these images looks slightly different.

In Figure 7(b), the 'background' has become significantly rougher [roughness of 23 nm, Fig. 7(c)] indicating that the foam material had changed the surface properties of the TP material. For samples with PU-a foam system peeled from the same PC/ABS-SMA TP material [Fig. 7(b)], the AFM pictures look similar, but also some larger foam parts ($\sim$ 0.25 to 0.5 μm in diameter) could be observed remaining on the TP surface after separating the foam. This should be connected to the higher peeling force, necessary to remove this foam from the interface. The roughness of the background (without larger foam parts) was once again with 28.4 nm slightly increased.

From AFM measurements, it was not possible to distinguish whether a thin layer of foam remains on the TP surface or if the TP surface has become rougher itself. The latter might be caused by the migration of unreacted isocyanate groups from PU foam mixture to the interface region followed by the formation of chemical linkages to the active hydrogen containing groups (e.g., hydroxyl group) on TP material surface[32,37–39] or some other interfacial reaction.[40,41] Dillingham and Moriarty[42] have studied the adhesion of isocyanate based polymers to steel where they found that the origin of excellent adhesion of polymers to steel is due to the formation of oxide-cyanate esters (analogous to urethane).

Observing the PU-b surface after being peeled from the TP material, holes in the PU foam surface can be seen, which are caused by the spherical particles from TP surface [Fig. 6(c)]. The deformation of the PU foam at the hole boundary can be related to a chemical interaction of PU foam with TP materials. Kieffer et al.[43,44] have also observed a similar behavior on interfacial reaction of polyurethanes with hydroxyl groups on cured epoxy.

X-ray photoelectron spectroscopy

The surface chemical composition of neat PC/ABS-SMA and from the separated PC/ABS-SMA, and PU-a interface after climate treatment and peeling was determined by XPS technique. The XPS results for all the samples show the presence of four elements: carbon, oxygen, nitrogen, and silicone. The atomic % data for investigated samples are given in Figure 8. The atomic % of carbon, oxygen, and nitrogen are quite different for the TP surface before foaming and after peeling. Furthermore, the elemental composition of TP material surface after peeling and the PU foam are nearly identical. This indicates that the main part of the TP surface after peeling the foam is dominated by the PU foam material.

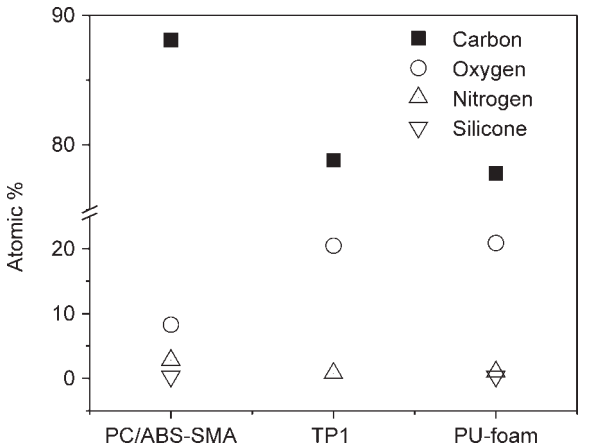

Figure 8 The elemental content from neat PC/ABS-SMA TP material, PC/ABS-SMA TP material from PU foam surface (TP1) and PU-a foam from PC/ABS-SMA TP material surface after climate treatment.

A significant difference in the bond structure between the foam and the TP surface was not observable; therefore no information on any chemical linkages between foam parts (e.g., MDI) and TP could be obtained.

Contact angle

The PU foam layer was removed from the TP material plates after climate treatment and the contact angle measurements were carried out on TP plate surface using a series of different liquids (see Experimental section for details). Figure 9 shows the surface tension data of the TP material plates before the foaming process was performed and also for four TP material plates after foaming, climate treatment, and adhesive peeling of the foam. (As the SMA sample did not show adhesive peeling even after climate treatment, no comparable surface tension data could be obtained.) In addition, the surface tension data for a PU-a foam surface is added, but here, as written in the Experimental part earlier, the foam was not peeled from the TP material. It can be seen from the Figure 9 that all the neat TP materials have slightly different surface tension, most significant in the polar part. But after foaming, climate treatment, and peeling of the foam, all surface tensions are nearly identical within the experimental error. The total surface tension for these samples was $\sim$ 46.8 $\pm$ 1 mN/m, the polar part $\sim$ 11.2 $\pm$ 1 mN/m. Compared to the surface tension of the foam material surface after peeling, the polar part is with 12.3 $\pm$ 1.5 mN/m in the same range, but the total surface tension with 40 $\pm$ 3 mN/m slightly smaller. But as the test liquids might seep

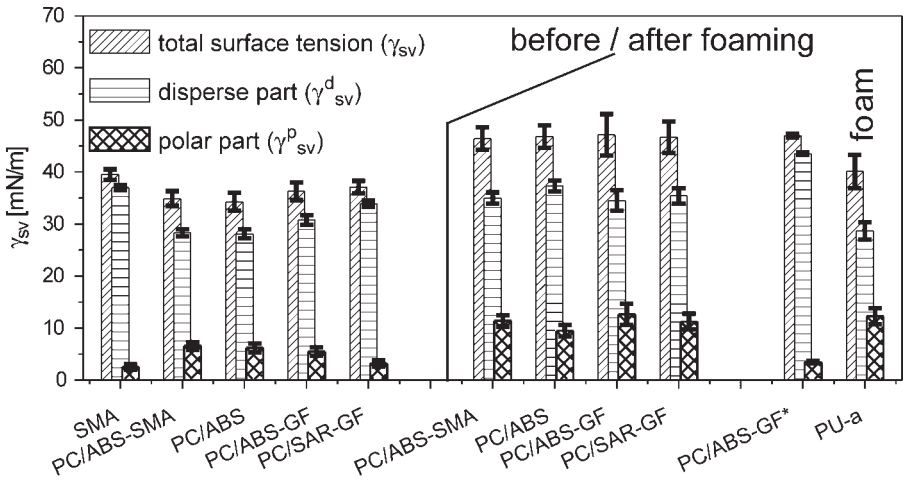

Figure 9 Surface tension data [total (γ_{sv}), polar (γ^p_{sv}), and disperse part (γ^d_{sv})] for TP materials before foaming and after separation from PU foam interface after climate treatment. Also the surface tension data for a PC/ABS-GF sample after drying (indicated by *) and for the PU-a foam surface (after peeling from PE) are given.

into the foam sample, the measured values of the surface tension of the foam could be too small.

In principle, a change in surface tension of TP materials separated from PU foam interface after climate treatment might have different causes:

1. some part of foam material left on the surface,
2. the surface has become more rough after removing from PU foam,
3. some additives have deposited on the surface (e.g., catalyst), and
4. water sorption during climate treatment.

To check the influence of these factors on surface tension, the PC/ABS-GF sample after peeling was blown with compressed air, washed with distilled water (without strong mechanical forces), and dried for 36 h at 50°C. The results are also shown in Figure 9. The total surface tension of the sample was not affected with washing and drying, however, the polar and disperse parts were changed significantly. The disperse part changed from 34.5 to 45.5 mN/m, while the polar part decreased from 12.7 to 3.5 mN/m. It shows that the sorbed water during climate treatments has been removed after drying the sample. In any case the results for interface sample (PC/ABS-GF) are not similar to that of neat PC/ABS-GF surface. Therefore, the foaming on TP material surface leads to similar change of the surface properties of all (PC based) TP materials in the same manner, and based on the XPS results, this is due to remaining PU material on the surface.

CONCLUSION

The adhesion behavior of three different types of PU foams with five different types of TP materials has been investigated. Two foam systems (PU-a and PU-b) have shown a good adhesion to all of the TP materials, when no aging by a thermal treatment was performed. The third foam, PU-c, has only shown a good adhesion to the SMA TP material. This was also the only TP material which has shown a good adhesion after thermal treatment of the PU-a and PU-b foam samples. An explanation for the good adhesion on SMA material might be a chemical linkage between isocyanate and MA, which gives imide linkage, but this assumption needs further investigations to be verified.

After thermal treatment, which lowers as an aging simulation the adhesion strength, the PU-a foam shows a slightly stronger adhesion when compared with the PU-b system, which can be related to their reactivity, but both foam materials have shown the same behavior in the further investigations.

By AFM measurements, an increase in surface roughness of the TP surface from ~ 7 to ~ 25 nm was observed, when the material after peeling the foam was compared with the neat material. Although in some cases, larger particles of foam (in the range of 0.5 μm) could be seen remaining on the surface, most parts of the surface look similar to the untreated sample.

Using XPS, the surface chemical composition of neat PC/ABS-SMA and of both sides of the separated PU-a foam/PC/ABS-SMA interface it could be determined, that the PU foam is dominating the surface composition of the PC/ABS-SMA material after separation. Contact angle measurements have verified this result for the other TP materials. As no (significant) foam particles were seen in AFM measurements, a thin layer of PU might cover the TP material, chemically linked to the surface. The thickness of this layer should be in the range of 15–20 nm to explain the increased roughness.

Even if the investigations could not help to clarify the adhesion mechanism itself, the results give a deeper insight in the failure mechanism of PU foams.

The authors thank Dr. R. Adhikari for carrying out AFM measurements.

References

1. Cooper, S. L.; Tobolsky, A. V. J Appl Polym Sci 1966, 10, 1837.
2. Briggs, D. Surface Analysis of Polymers by XPS and Static SIMS; Cambridge University Press: New York, 1998.
3. Chan, C. M. Polymer Surface Modification and Characterization; Hanser: New York, 1994.
4. Offord, D. A.; John, C. M.; Linford, M. R.; Griffin, J. H. Langmuir 1994, 10, 883.
5. Davies, M. C.; Lynn, R. A. P.; Davis, S. S.; Hearn, J.; Watts, J. F.; Vickerman, J. C.; Johnson, D. J Colloid Interface Sci 1993, 156, 229.
6. Vanden Eynde, X.; Bertrand, P.; Dubois, P.; Jerome, R. Macromolecules 1998, 31, 6409.
7. Vanden Eynde, X.; Bertrand, P. Surf Interface Anal 1998, 26, 579.
8. Leeson, A. M.; Alexander, M. R.; Short, R. D.; Briggs, D.; Hearn, M. J. Surf Interface Anal 1997, 25, 261.
9. Li, L.; Ng, K. M.; Chan, C. M.; Feng, J. Y.; Zeng, X. M.; Weng, L. T. Macromolecules 2000, 33, 5588.
10. Li, L.; Chan, C. M.; Weng, L. T.; Xiang, M. L.; Jiang, M. Macromolecules 1998, 31, 7248.
11. Briggs, D.; Davies, M. C. Surf Interface Anal 1997, 25, 725.
12. Briggs, D.; Ratner, B. D. Polym Commun 1988, 29, 6.
13. Taunton, H. J.; Toprakcioglu, C.; Fetters, L. J.; Klein, J. Nature 1988, 332, 712.
14. Kinloch, A. J.; Lau, C. C.; Williams, J. G. Int J Fract 1994, 66, 45.
15. Kendall, K. J Adhes 1973, 5, 105.
16. Kim, K. S.; Aravas, N. Int J Solid Struct 1988, 24, 417.
17. Kinloch, A. J.; Williams, J. G. In Adhesion Science and Engineering-1: The Mechanisms of Adhesion; Dillard, D. A.; Pocius, A. V., Eds.; Elsevier: Amsterdam, 2002; p 273.
18. Blackman, B. R. K.; Kinloch, A. J.; Paraschi, M.; Teo, W. S. Int J Adhes Adhes 2003, 23, 293.
19. Kinloch, A. J. Proc Inst Mech Eng Part G 1997, 211, 307.
20. Blackman, B. R. K.; Hadavinia, H.; Kinloch, A. J.; Williams, J. G. Int J Fract 2003, 119, 25.
21. Georgiou, I.; Hadavinia, H.; Ivankovic, A.; Kinloch, A. J.; Tropsa, V.; Williams, J. G. J Adhes 2003, 79, 239.
22. Mahmood, N.; Kressler, J.; Busse, K. J Appl Polym Sci 2005, 98, 1280.
23. Colvin, B. G. Cell Polym 1992, 11, 29.
24. Lowe, D. W.; Arai, S. J Cell Plast 1987, 23, 33.
25. Kaushiva, B. D.; Wilkes, G. L. Polymer 2000, 41, 6981.
26. Good, R. J. J Adhes Sci Technol 1992, 6, 1269.
27. Girifalco, L. A.; Good, R. J. J Phys Chem 1957, 6, 904.
28. (a) Rabel, W. Farbe und Lack 1971, 77, 997. (b) Owens, D. K.; Wendt, R. C. J Appl Polym Sci 1969, 13, 1741.
29. Ström, G.; Fredriksson, M.; Stenius, P. J Colloid Interface Sci 1987, 119, 352.
30. Fowkes, F. M. J Ind Eng Chem 1964, 56, 40.
31. Gebhard, K. F. Grundlagen der physikalischen Chemie von Grenzflächen und Methoden zur Bestimmung geometrischer Größen: FHG IGB Stuttgart, 1982.
32. Gutman, L.; Chakraborty, A. K. J Chem Phys 1995, 103, 10733.
33. Liao, D. C.; Hsieh, K. H. J Polym Sci Part A: Polym Chem 1994, 32, 1665.
34. Möginger, B.; Michler, G. H.; Ludwigs, H.-C. In Deformation and Fracture Behavior of Polymers; Grellmann, W.; Seidler, S., Eds.; Springer-Verlag: Berlin, 2001; p 335.
35. Keisler, C.; Lataillade, J. L. J Adhes Sci Technol 1995, 9, 395.
36. Sancaktar, E.; Gomatam, R. J Adhes Sci Technol 2001, 15, 97.
37. Gutman, L.; Chakraborty, A. K. J Chem Phys 1994, 101, 10074.
38. Brown, H. R.; Russell, T. P. Macromolecules 1996, 29, 798.
39. Shaffer, J. S. Macromolecules 1995, 28, 7447.
40. Dillingham, R. G.; Moriarty, C. J Proc Annu Meet Adhes Soc 2002, 25, 316.
41. Lee, I.; Wool, R. P. Macromolecules 2000, 33, 2680.
42. Dillingham, R. G.; Moriarty, C. J Adhes 2003, 79, 269.
43. Kieffer, A.; Hartwig, A.; Schmidt-Naake, G.; Hennemann, O.-D. Acta Polym 1999, 49, 720.
44. Kieffer, A.; Hartwig, A. Macromol Mater Eng 2001, 286, 254.